Helix-Forming Oligoureas: Temperature-Dependent NMR, Structure Determination, and Circular Dichroism of a Nonamer with Functionalized Side Chains

by **Christine Hemmerlin** and **Michel Marraud**

LCPM, UMR CNRS-INPL 7568, ENSIC-INPL, B.P. 451, F-54001 Nancy

and

Didier Rognan

Laboratoire de Pharmacochimie de la Communication Cellulaire, UMR CNRS, ULP 7081, 74 Route du Rhin, B.P. 24, F-67401 Illkirch

and

Roland Graff

Faculté de Chimie, 1 Rue Blaise Pascal, F-67008 Strasbourg

and

Vincent Semetey[1]), **Jean-Paul Briand,** and **Gilles Guichard***

Immunologie et Chimie Thérapeutiques, UPR CNRS 9021, Institut de Biologie Moléculaire et Cellulaire, 15 Rue Descartes, F-67084 Strasbourg

Dedicated to Professor *Dieter Seebach* on the occasion of his 65th birthday

To further investigate the degree of structural homology between γ-peptides **A** and *N,N′*-linked oligoureas **B**, we prepared oligourea nonamer **2** containing Ala, Val, Leu, Phe, Tyr and Lys side chains. Oligomer **2** was synthesized on solid support from activated monomers, *i.e.*, from enantiomerically pure succinimidyl {2-{[(9*H*-fluoren-9-ylmethoxy)carbonyl]amino}ethyl}carbamates **3a**–**f** that are further substituted at C(2) of the ethyl moiety. These precursors were conveniently prepared from *N*-Fmoc-protected β^3-amino acids with corresponding side chains. Detailed NMR studies (DQF-COSY, TOCSY, and ROESY) in (D_5)pyridine revealed that **2** adopts a regular (*P*)-*2.5* helical secondary structure very similar to that previously determined for oligourea heptamer **1** and closely related to the (*P*)-2.6_{14} helix of γ-peptides. Temperature-dependent NMR further demonstrated the conformational homogeneity and remarkable stability of the structure of **2** in pyridine. The CD spectrum of **2** (0.2 mM) was recorded in MeOH with the aim to gain more information about the conformation of oligoureas. In contrast to *2.6*-helical γ-peptides, which display only a weak or no *Cotton* effect, oligourea **2** exhibits an intense positive *Cotton* effect at *ca.* 203 nm ($[\Theta] = +373000$ deg cm^2 dmol^{-1}) that decreases only slowly upon increasing the temperature.

Introduction. – Inspired by the unique three-dimensional structures of biomacromolecules (*e.g.*, proteins, nucleic acids), chemists are now creating synthetic oligomeric materials ('artificial bio-oligomers') in which enough conformational control can lead to the formation of well-defined secondary structures stabilized by noncovalent interactions [1]. In the field of peptidomimetics, seminal work by *Seebach* and co-

[1]) New address: Department of Chemistry and Chemical Biology, Harvard University, 12 Oxford Street, Cambridge, MA 02138, USA.

workers [2–4], *Gellman* and co-workers [5][6], and *Hanessian* and co-workers [7] has demonstrated that properties such as folding and structural diversity are not restricted to natural α-polypeptides but are shared by synthetic peptides consisting exclusively of higher ω-amino acids such as β- and γ-amino-acids[2]). Indeed, short-chain β- and γ-peptides with defined substitution patterns can form stable helices [2][4a][5][7a], sheets [3][6], and turns [3][4d][6][7b] in solution and in the solid state. Since this early work, some reports have highlighted the potential of other ω-amino acids including conformationally restricted δ-amino acids (*e.g.*, sugar amino acids) for the construction of folding oligomers [9]. Interestingly, within each ω-peptide subclass, isosteric backbone modifications can be introduced to generate peptidomimetics that, in turn, might well form stable and novel secondary structures. Although the syntheses of a number of such oligomeric peptidomimetics have been described in the literature, detailed conformational analyses demonstrating unambiguously the presence of regular secondary structures have been limited to a few[3]).

The substitution of a heteroatom for the C(α) or C(ω) of the amino acid constituents of ω-peptides represent an interesting modification that has been used to generate α-[13], β-[12][14], and γ-peptide [15][16] mimetics. In these systems, the degree of structural homology with the reference ω-peptide is somewhat difficult to predict, and the answer needs detailed case-by-case conformational investigation. For example, oligomers (as short as trimers) of α-aminooxy acids obtained by replacement of the C(β) of each residue of β-peptides with an O-atom adopt a twisted 2_8 helical structure in solution [12], whereas the corresponding β^2-peptides exhibit a 3_{14} helical secondary structure. Conversely, *ab initio* calculations conducted on hydrazinopeptides (*i.e.*, the C(β) of each residue within a β-peptide is substituted with an N-atom) revealed a variety of secondary structures including a highly stable *3.3*-helical structure that topologically differs from the 3_{14} helix [14a][4])

We have recently started a program aimed at studying the conformational preference of urea-based peptidomimetics [17–19]. In this context, we postulated that the replacement of the C(α) of γ-amino acid residues by an N-atom in the backbone of γ-peptides of type **A**, which generates *N*,*N*′-linked oligoureas of type **B**[5]),

A **B**

---

[2]) For reviews on β-peptides, see [8].

[3]) α-Peptide mimetics that have been shown to form helical secondary structure in solution include oligo(*N*-substituted glycines) with α-chiral aromatic side chains [10], and conformationally restricted polyimides (homo-oligomers of L-pyroglutamic acid) [11]. Oligomers of α-aminooxy acids that belong to the β-peptide lineage have also been found to fold into helical structure [12].

[4]) However, although preliminary CD studies have been performed on hydrazinopeptides [14b], experimental data to ascertain these predictions are still needed.

[5]) These oligomers were initially synthesized by *Burgess* and co-workers [15].

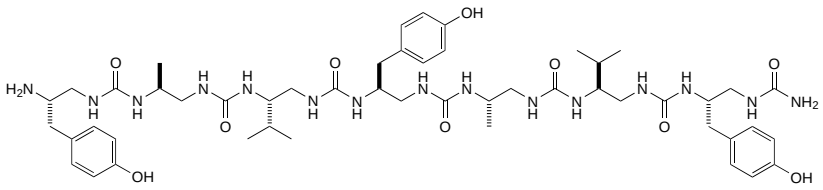

1

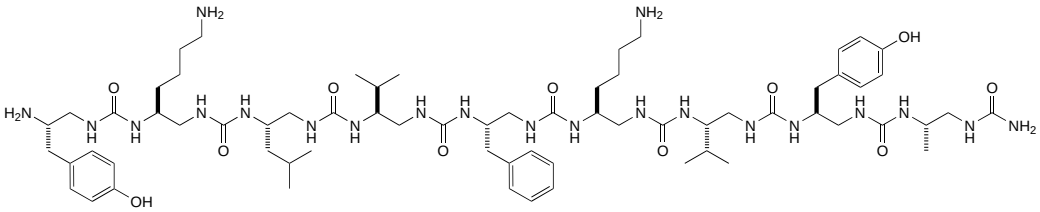

2

was compatible with the *2.6* helical backbone of γ-peptides. NMR Structure determination in (D_5)pyridine of heptamer **1** with Ala, Val, and Tyr side chains confirmed that most of the structural information encoded in the reference γ-peptide was preserved upon heteroatom substitution (*Fig. 1*). Heptamer **1** was shown to adopt a right-handed *2.5* helix of 5.1 Å pitch characterized by the presence of 12- and 14-membered H-bonded pseudocycles [18].

To gain further insight into the conformational preferences of *N*,*N*′-linked oligoureas and learn about the influence of the sequence on the folding, we prepared nonamer **2** with Ala, Val, Leu, Phe, Tyr, and Lys side chains and performed a detailed conformational analysis in solution.

2. Preparation of Oligourea 2. – *N*,*N*′-Linked oligoureas are readily accessible by solid-phase-synthesis methodology with a variety of appropriate monomers. Originally, *Burgess* and co-workers utilized enantiomerically pure 2-phthalimido-1-substituted ethyl isocyanates prepared by treatment of the corresponding 2-phthalimido-1-substituted ethylamines with phosgene [15]. A number of alternative building blocks including activated carbamates have since been proposed (*e.g.*, 4-nitrophenyl (2-azido-1-X-ethyl)carbamates [20], 4-nitrophenyl {2-{[(*tert*-butoxy)carbonyl]amino}-2-X-ethyl}-carbamates [21], or succinimidyl {2-{[(*tert*-butoxy)carbonyl]amino}-2-X-ethyl}carbamates [22]). Because of the utility of the *N*-Fmoc protecting group in the solid-phase synthesis of peptides, we have recently described the preparation of succinimidyl {2-{[(9*H*-fluoren-9-ylmethoxy)carbonyl]amino}-2-X-ethyl}carbamates as novel building blocks for the synthesis of oligoureas on solid support [23]. Enantiomerically pure *N*-Fmoc-protected succinimidyl carbamates **3a**–**f** with Ala, Val, Leu, Phe, Tyr, and Lys side chains required for the synthesis of **2** were prepared as previously described starting from *N*-Fmoc-β^3-amino acids.

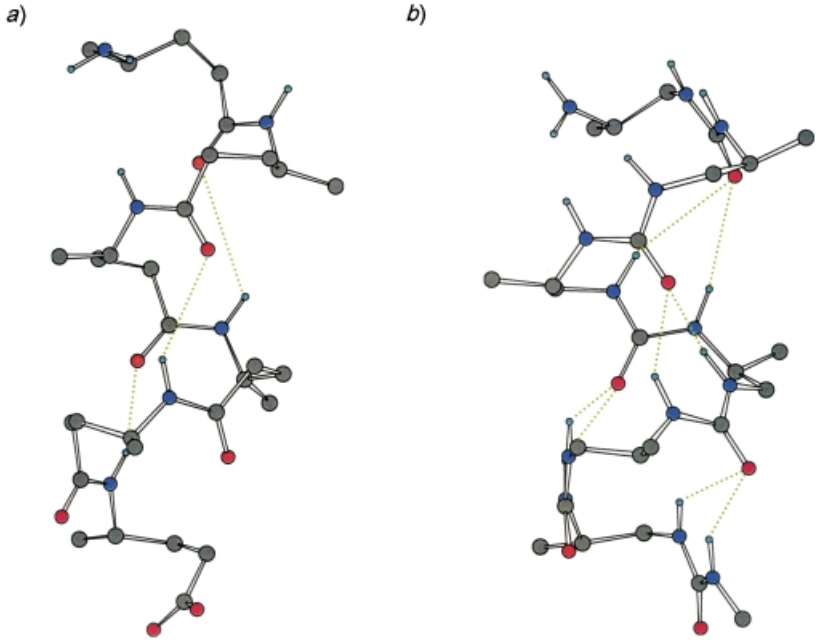

Fig. 1. *Comparison of the helical secondary structures and H-bonding patterns of* a) *γ-peptides* **A** *and* b) N,N′-*linked oligoureas* **B**. *a*) Side view of the right-handed 2.6_{14} helix with a pitch of 5.0 Å formed by γ^4-peptides in solution as determined by NMR in (D_5)pyridine (adapted from [4a]). The structure is stabilized by C=O(i)$\cdots$H–N($i+3$) H-bonds that close 14-membered H-bonded rings. *b*) Side view of the right-handed *2.5* helical secondary structure of oligoureas. The structure depicted is a section of the NMR structure of heptaurea **1** determined in (D_5)pyridine [18]. The helix has a pitch of *ca.* 5.1 Å and is characterized by the simultaneous presence of C=O(i)$\cdots$H–N′($i+2$) and C=O(i)$\cdots$H–N($i+3$) H-bonds that close 12- and 14-membered H-bonded rings, respectively.

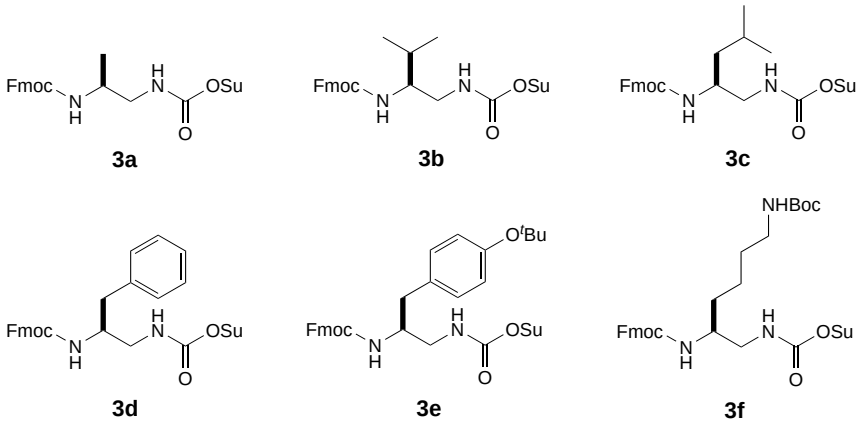

Briefly, *N*-Fmoc-β^3-Xaa-OH [24] were first converted to the corresponding acyl azides, and, following *Curtius* rearrangement, the resulting isocyanates were treated with *N*-hydroxysuccinimide to give carbamates **3a**–**f** in good yields (51–86%). Carbamates **3a**–**f** are white solids that can be stored for months at 4° or at room temperature without degradation. Nonamer **2** was assembled on *Rink* amide resin [25] *via* successive coupling and deprotection cycles (see *Scheme*). The purity of the crude oligomer, obtained after cleavage from the resin and lyophilization was 32% as checked by reversed-phase HPLC. Oligomer **2** was purified by reversed-phase HPLC (C_{18}) to a final purity > 95% and lyophilized.

Scheme. *Synthesis of Oligourea* **2** *on Solid Support*

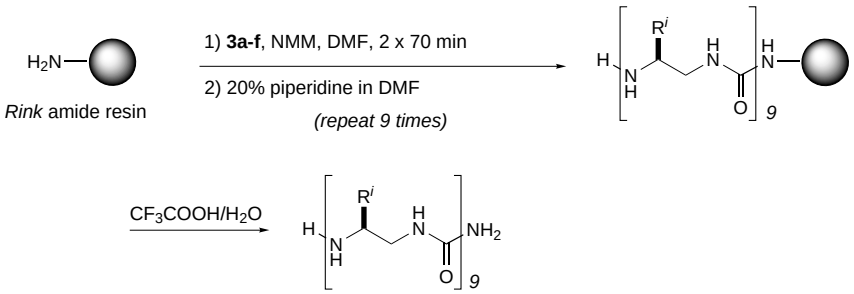

3. Temperature-Dependent NMR and Structure Determination of 2 in (D_5)Pyridine. – The NMR conformational analysis of **2** was conducted in a manner analogous to that previously described for **1** [18]. The choice of (D_5)pyridine as a solvent was dictated by the larger dispersion and better resolution observed particularly in the NH region compared to CD_3OH[6]). The consequences were: *i*) an easier identification of spin systems for all residues, *ii*) the access to ^3J(NH,H–C(β)) for residues 2–9 as well as to some ^3J(N′H$_{si}$–C(α)) and ^3J(N′H,H$_{Re}$–C(α)), *iii*) the possibility to study temperature dependence over a large range of temperature (80 K).

DQF-COSY and TOCSY Measurements allowed the assignment of proton resonances for all residues. The chemical shifts are collected in *Table 1*. In the fingerprint NH/H–C(β) and N′H$_{si}$–C(α) region (for stereospecific assignment of diastereotopic C(α) protons, *vide infra*) of the DQF-COSY experiment recorded at 308 K, almost all cross-peaks were properly resolved (*Fig. 2*). Interestingly, N′H of residues 4–9 appear systematically downfield with respect to the corresponding NH, while the opposite is observed for residues 2 and 3[7]). Unequivocal sequence-specific assignment was accomplished by analysis of short range N′H(i)/NH($i+1$) NOE connectivities in the ROESY experiment recorded at 308 K ($\tau_m = 300$ ms).

---

[6]) The original conformational analyses of γ-peptides reported independently by the groups of *Seebach* [4a] and *Hanessian* [7a] were also carried out in (D_5)pyridine.

[7]) Residues in **2** were numbered consecutively from 1 to 9 starting from the amino-terminal residue with a Tyr side chain.

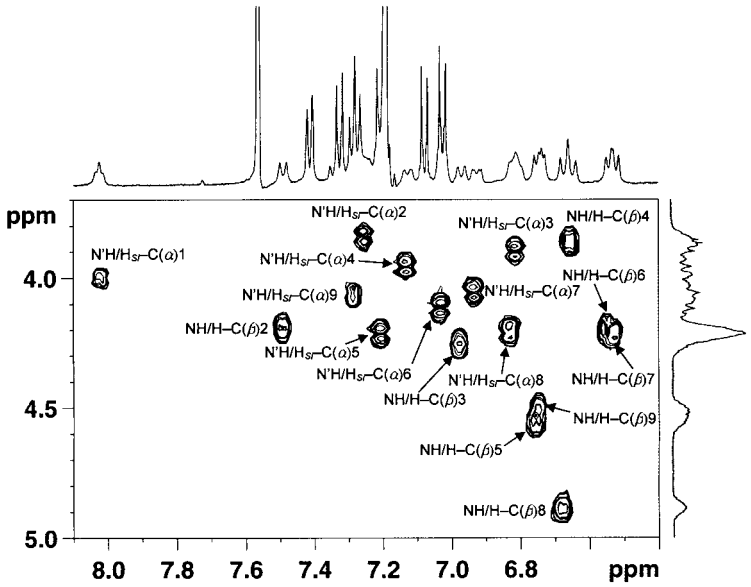

Fig. 2. *Fingerprint* NH/H–C(β) *and* N′H/H_{Si}–C(α) *region of the DQF-COSY experiment of* **2**, *recorded at 308 K in* (D_5)*pyridine.* Residues are numbered consecutively from 1–9 starting from the amino-terminal residue with the Tyr side chain.

Table 1. *^{1}H-NMR Chemical Shifts* [ppm] *of Nonamer* **2** *in* (D_5)*Pyridine*

Residue	NH	N′H	H–C(β)	H_{Si}–C(α)	H_{Re}–C(α)	H–C(γ)	Others
1	–	8.01	4.23	4.01	3.59	3.39, 3.20	7.33 (H_o)
							7.09 (H_m)
2	7.48	7.25	4.20	3.85	2.79	1.98, 1.89	1.53 (H–C(δ))
							1.60 (H–C(ε))
							3.31 (H–C(ξ))
3	6.97	6.81	4.26	3.91	2.60	1.88, 1.32	1.14 (H–C(δ))
							0.95 (H–C(ε))
4	6.66	7.13	3.86	3.95	2.59	1.59	0.96 (H–C(δ))
5	6.76	7.20	4.55	4.22	2.86	2.86, 2.78	7.19 (H_o)
							7.41 (H_m)
							7.29 (H_p)
6	6.55	7.03	4.21	4.11	2.64	1.88, 1.72	1.34 (H–C(δ))
							1.50 (H–C(ε))
							3.24 (H–C(ξ))
7	6.54	6.93	4.22	4.05	2.65	1.70	1.21, 0.90 (H–C(δ))
8	6.68	6.83	4.88	4.21	2.72	2.72	7.33 (H_o)
							7.09 (H_m)
9	6.75	7.28	4.51	4.08	3.18	1.15	–

Qualitative comparison of ^{1}H-NMR spectra of **2** and **1** recorded in (D_5)pyridine revealed a number of striking similarities. These include large ^3J(NH,H–C(β)) values, large chemical-shift differences between diastereotopic H–C(α) protons for central residues, strong differentiation between vicinal coupling constants of each pair of

diastereotopic H–C(α) along the sequence, as well as very little temperature dependence for these parameters. Taken together, these data represent indicators of conformational homogeneity [26] as well as of conformational similarity with **1**.

The ^3J(NH,H–C(β)) values extracted from the ^{1}H-NMR spectra of **2** recorded between 292 and 362 K with 10 K increments are collected in *Table 2*. For residues 3–8, these values are not significantly affected by temperature and remain $\geq$10 Hz even at 362 K. This is consistent with a highly stable *anti*-periplanar arrangement of NH and H–C(β)[8]). The coupling constants of flanking residues 2 and 9 have slightly smaller values (8–10.2 Hz) within the same temperature range.

Table 2. *Variation of ^{3}J(NH,H–C(β)) Values of Residues* 2–9 *of Nonamer* **2** *upon Temperature Increase from 292 to 362 K.* n.d. = not detected.

Temperature [K]	Residue number *i*							
	2	3	4	5	6	7	8	9
292	n.d.	n.d.	10.2	10.5	10.2	10.2	10.2	8.5
302	n.d.	n.d.	10.4	10.4	10.2	10.5	10.2	8.5
312	9.2	10.5	10.7	10.8	10.8	10.7	10.7	9.7
322	10.2	10.4	10.4	10.4	10.4	10.8	10.7	8.9
332	n.d.	10.2	10.4	10.4	10.4	10.4	10.5	8.4
342	n.d.	10.2	10.4	10.4	10.2	10.4	10.2	8.0
352	n.d.	10.5	10.4	10.5	10.5	10.7	10.4	8.4
362	9.5	10.0	10.5	10.2	10.5	10.5	10.5	n.d.

At first sight, the COSY and TOCSY experiments of **2** reveal that the two geminal C(α) protons for residues 2–9 display markedly different spectroscopic behaviors. The differences in chemical shifts ($\Delta\delta$) determined for each residue between 286–362 K is reported in *Table 3*. In the case of residues 3–8, this difference is large ($1.37 < \Delta\delta <$ 1.53 ppm at 286 K) and decreases only slowly upon increasing the temperature ($1.29 < \Delta\delta < 1.45$ ppm at 362 K)[9]). Smaller $\Delta\delta$ values were measured for residue 1 ($\Delta\delta <$ 0.45 ppm), and, to a lesser extent, for residues 2 ($\Delta\delta \leq 1.1$ ppm) and 9 ($\Delta\delta < 1$ ppm). $\Delta\delta$ Values of flanking residues 1 and especially 9 are the most sensitive to variations of temperature. Nevertheless, the nonequivalence of diastereotopic C(α) protons within residues 2–8 at high temperature is consistent with their location in a distinct spatial environment that is not affected by temperature changes and, thus, confirms the existence of a well-defined and stable secondary structure. The conformation around the C(α)–C(β) bond was then examined in more details.

Fig. 3 shows *Newman* projections along the C(α)–C(β) bond for the three possible conformers **I**–**III** with experimental requirements to be fulfilled so as to validate one form or another. The exact measurement of ^3J(H–C(β),H–C(α)) values was not possible due to overlap of H–C(β) resonances. However, careful examination of DQF-COSY data obtained between 282–362 K qualitatively indicates that, for all residues, the downfield C(α) proton exhibits a small coupling constant with H–C(β) (the corresponding cross-peaks were not detectable in the DQF-COSY plot), whereas the

[8]) Similarly, in the case of β- and γ-peptides, the rotation is highly restricted around N–C(β) and N–C(γ) bonds, respectively, and the corresponding protons are situated in a nearly *anti*-periplanar arrangement.

[9]) In our previous study of heptamer **1**, $\Delta\delta$ values measured for central residues 3–6 were in the same range.

Table 3. *Chemical-Shift Differences* ($\Delta\delta$) *Between Geminal C(α) Protons for Residues 1–9 of Oligomer* **2** *as Determined from DQF-COSY Experiments Recorded in (D_5)Pyridine between 282 to 362 K*

Temperature [K]	Residue number *i*								
	1	2	3	4	5	6	7	8	9
282	0.43	1.11	1.37	1.39	1.38	1.53	1.39	1.52	0.97
292	0.42	1.10	1.32	1.37	1.37	1.51	1.40	1.50	0.94
302	0.40	1.08	1.31	1.37	1.38	1.50	1.40	1.47	0.90
312	0.41	1.05	1.30	1.36	1.36	1.48	1.41	1.46	0.86
322	0.40	1.05	1.30	1.36	1.35	1.47	1.41	1.43	0.83
332	0.39	1.03	1.30	1.35	1.35	1.47	1.41	1.40	0.79
342	0.38	1.00	1.29	1.35	1.34	1.45	1.41	1.38	0.75
352	0.36	0.99	1.28	1.34	1.33	1.44	1.41	1.35	0.72
362	0.35	0.98	1.29	1.34	1.34	1.45	1.41	1.32	0.69

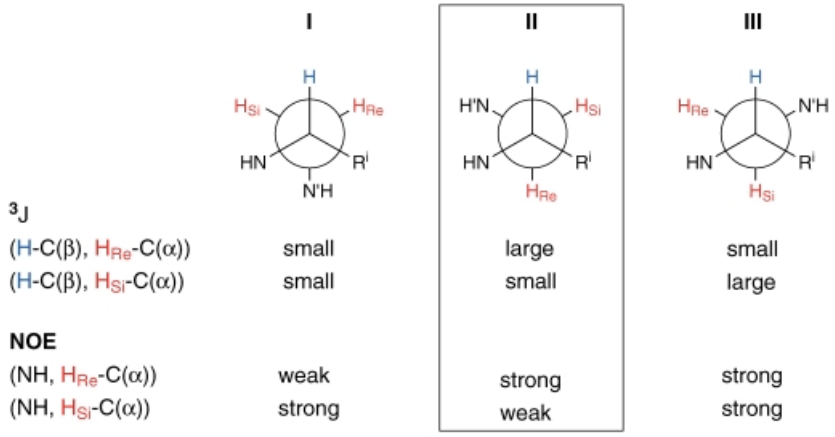

Fig. 3. *Representation of the three possible conformers* **I**–**III** *along the* C(α)–C(β) *bond in* Newman *projection together with required NMR criteria to validate one particular conformation*. Measurements of ^3J(H–C(β),H–C(α) coupling constants and intensities of intra-residue NOE between NH and C(α) protons in **2** indicate that exclusively conformer **II** is populated and that the downfield C(α) proton corresponds to H_{Si}–C(α).

upfield C(α) proton has a large coupling constant with H–C(β). Hence, conformer **I** can be excluded. Comparison of intra-residue NOE intensities between NH and both H–C(α) protons for residues 2–9 reveals that the downfield C(α) proton consistently displays a weaker NOE to NH than the corresponding upfield C(α) proton (exemplified for residue 2 in *Fig. 4*). This result excludes the possibility to have conformer **III** populated, and confirms that form **II** is the only one to be in full agreement with experimental data (this is verified for all residues but 1). In addition, this careful examination allowed the unambiguous stereospecific attribution of diastereotopic C(α) protons, the downfield proton being assigned to H_{Si}–C(α).

Extraction of ^3J(N′H,H–C(α)) values to gain information on the conformational restriction around the N′–C(α) bond was problematic because of severe overlap of the aromatic protons of **2** with residual pyridine protons. Qualitative examination of DQF-

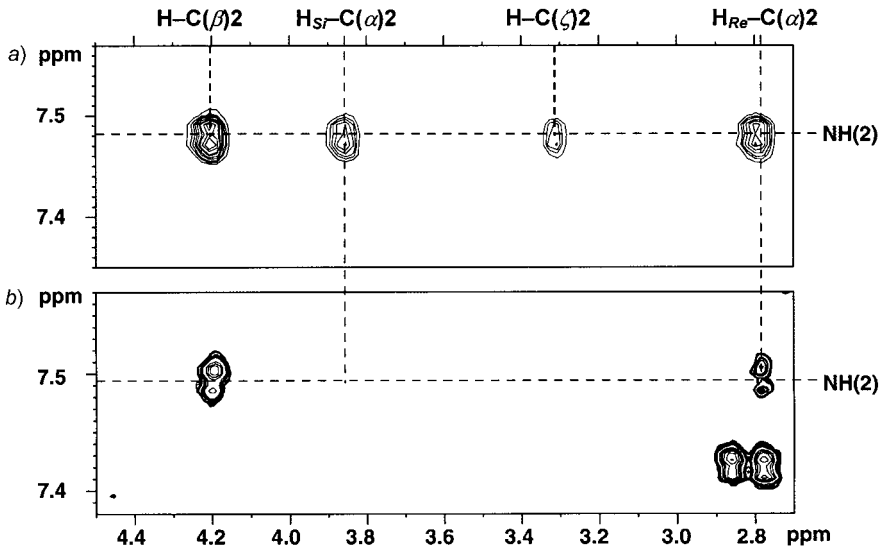

Fig. 4. *Parts of the* a) *TOCSY and* b) *ROESY plots showing cross-peaks between NH and* C(α) *protons of residue 2*. Strong NOE cross-peaks are observed in the ROESY plot ($\tau_m = 300$ ms) between NH and H–C(β) as well as between NH and H_{Re}–C(α). These data, together with the absence of a significant NH/H_{Si}–C(α) NOE cross-peak, exclude the possibility to have conformer **III** (see *Fig. 3*) populated. Similar results were obtained for other residues.

COSY data recorded between 292–362 K revealed that, for all residues except residue 1, H_{Si}–C(α) exhibits a large coupling constant with N′H, while the H_{Re}–C(α) has a small one (the N′H/H_{Re}–C(α) cross-peaks were hardly detectable in the DQF-COSY plot). Still, decoupling experiments performed by irradiation of H_{Si}–C(α) or H_{Re}–C(α) at chosen temperatures between 295 and 329 K allowed the determination of ^3J(N′H,H–C(α)) values for residues 1, 2, 4–7, and 9. With the exception of residue 1 (^3J(N′H,H_{Si}–C(α)) = ^3J(N′H,H_{Re}–C(α)) = 5 Hz), ^3J(N′H,H_{Si}–C(α)) and ^3J(N′H,H_{Re}–C(α)) were between 7.4–10.5 Hz and 1–2 Hz, respectively, implying for these residues that N′H is nearly *anti*-periplanar to H_{Si}–C(α) and *syn*-clinal to H_{Re}–C(α).

As for α- [27] and β-peptides [2e], information about the solvent accessibility of NH protons in **2** and their possible engagement in H-bonds can be obtained from temperature coefficients. It is generally assumed that, for peptides in a rigidly folded state, amide protons with a temperature coefficient less negative than -4 ppb/K are involved in H-bonding. *Table 4* shows the temperature coefficients of the urea proton resonances determined for residues 1–9 over a range of 58.5 K. All NH signals shift upfield upon warming and thus display negative temperature gradients. Absolute values of temperature coefficients are ≥ 6.9 Hz in the case of the first two urea bonds, thus indicating high solvent accessibility. The values are very similar for both NH and N′H protons within these urea bonds (compare $-\Delta\delta/\Delta T$ of N′H(1) and NH(2)). In contrast, the particularly low absolute values determined for NH of residues 4–9 ($3.6 \geq -\Delta\delta/\Delta T \geq 2$) suggest solvent shielding and intramolecularly H-bonded protons.

Table 4. *Calculated Temperature Coefficients* $-\Delta\delta/\Delta T$ [ppb/K] *of NH*(i) *and N′H*(i) *Protons for* i = *1–9, in (D₅)Pyridine*

	Residue number *i*								
	1	2	3	4	5	6	7	8	9
NH (*i*)	–	9	6.9	3.5	2	2	3.1	2.3	3.6
N′H(*i*)	9	7	3.9	5.6	5.6	4.4	5.2	4.4	5.6

For $i = 3-9$, absolute values of temperature coefficients of N′H(i) are systematically higher than those of NH($i+1$). Although the same trend was observed for heptamer **1**, the difference contained between 0.4 and 2.6 ppb/K is probably not large enough (particularly in the case of the third, sixth, and eighth urea bond) to distinguish an increased solvent accessibility of N′H(i) compared to NH($i+1$).

The ROESY data obtained at 308 K ($\tau_m = 300$ ms) was selected to determine the three-dimensional structure of **2**. A total of 134 NOEs (interresidue and intraresidue) were extracted and classified according to their cross-peak volume in three categories: strong, medium, and weak. The 21 inter-residue NOEs (7 sequential, 12 with $(j-i)=2$, and 2 with $(j-i)=3$) are collected in *Table 5*.

Table 5. *Interresidue NOEs Observed in the ROESY NMR Plot* ($\tau_m = 300$ ms) *of Nonamer* **2**, *in (D₅)Pyridine at 308 K*

H-Atom	Residue *i*	H-atom	Residue *j*	NOE[a])	$k = j-i$
H_m	1	H–C(δ)	4	*s*	3
H_o	1	H–C(δ)	4	*m*	3
N′H	2	NH	3	*s*	1
N′H	3	NH	4	*s*	1
H–C(β)	3	NH	5	*s*	2
H–C(β)	3	N′H	5	*s*	2
N′H	4	NH	5	*s*	1
H–C(β)	4	NH	6	*s*	2
H–C(β)	4	N′H	6	*s*	2
H_{Si}–C(α)	4	N′H	6	*s*	2
N′H	5	NH	6	*s*	1
H–C(β)	5	NH	7	*s*	2
H–C(β)	5	N′H	7	*s*	2
H–C(β)	5	H_{Re}–C(α)	7	*m*	2
H_m	5	H_{Re}–C(α)	7	*m*	2
N′H	6	NH	7	*s*	1
H_{Si}–C(α)	6	N′H	8	*s*	2
N′H	7	NH	8	*s*	1
H_{Si}–C(α)	7	N′H	9	*m*	2
H–C(δ^2)	7	H_{Re}–C(α)	9	*s*	2
N′H	8	NH	9	*s*	1

[a]) Strong (*s*), <2.8 Å; medium (*m*), <3.8 Å; weak (*w*), <5.5 Å.

Medium-range connectivities of the type H–C(β)*i*/NH($i+2$), H–C(β)*i*/N′H($i+2$), and H_{Si}–C(α)(i)/N′H($i+2$) are particularly informative. Two regions of the ROESY plot containing the representative set of $i/(i+2)$ NOE connectivities between residues

4 and 6 are shown in *Fig. 5*. This NOE pattern repeated along the sequence and also found in the ROESY plot of heptamer **1** is consistent with the presence of a helical conformation. However, in contrast to what was previously observed with **1**, a number of $i/(i+2)$ NOE connectivities (between residues 2 and 4, 6 and 8, and 7 and 9) could not be assigned unequivocally because of resonance overlaps and, thus, were not used in the calculations.

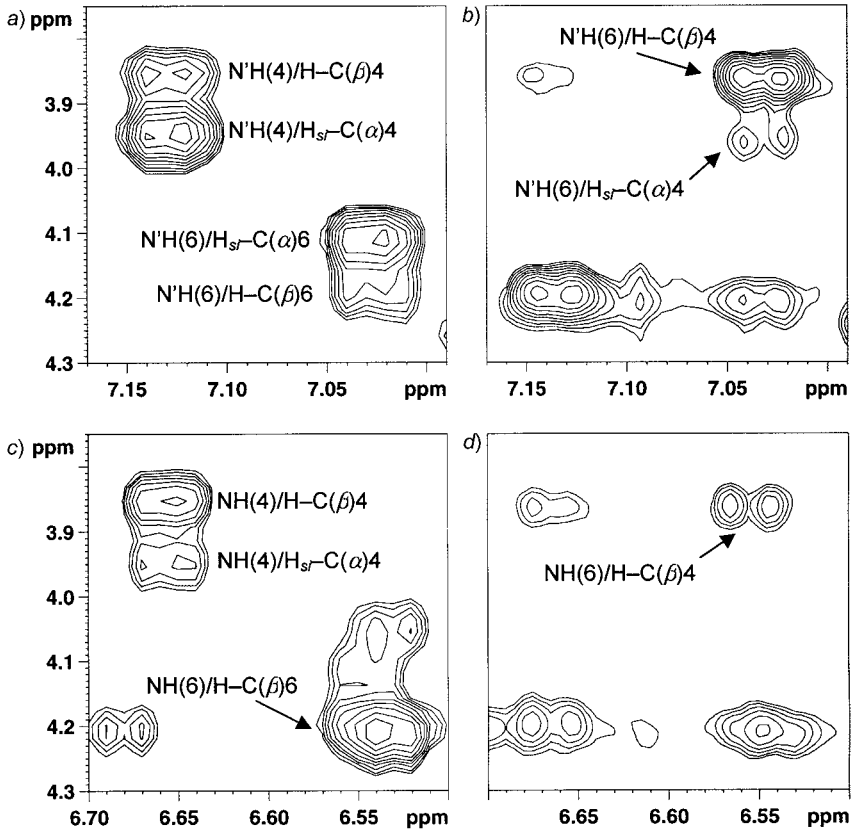

Fig. 5. *Representative set of* i/i+*2 NOE connectivities between residues 4 and 6 extracted from the ROESY plot* ($\tau_m = 300$ ms) *of* **2**. *a*) Part of the TOCSY plot showing N′H/H−C(β) and N′H/H_{Si}−C(α) cross-peaks for residues 4 and 6. *b*) ROESY plot with inter-residue N′H(6)/H−C(β)4 and N′H(6)/H_{Si}−C(α)4 . *c*) Part of the TOCSY plot showing NH/H−C(β) and NH/H_{Si}−C(α) cross-peaks for residues 4 and 6. *d*) ROESY plot with inter-residue NH(6)/H−C(β)4 NOE cross-peaks. These $i/i+2$ NOE connectivities, which are found for $i = 3, 5, 6$, and 7, are consistent with **2** adopting a regular helical structure.

The conformational analysis of nonamer **2** was further investigated by restrained molecular-dynamics calculations. A 100-ps simulated annealing refinement of 30 randomly chosen starting structures, under experimental NMR restraints (distance and dihedral-angle restraints), converged towards a regular right-handed *2.5* helix (well defined from residues 1–9) of *ca.* 5.1 Å pitch (the overall length of the helix is *ca.* 18 Å). The resulting structures show no NOE-violations greater than 0.50 Å and

dihedral-angle violations greater than 10°. The superimposition of the 20 lowest-energy structures is represented in *Fig. 6*.

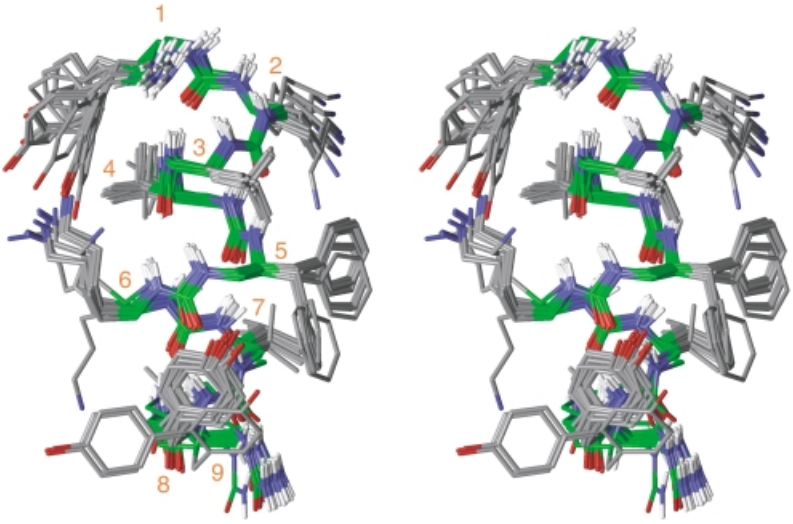

Fig. 6. *NMR Structure of oligourea* **2** *in (D5)pyridine* (stereo view along the helix axis). Bundle of the 20 best structures of lowest energy. Root-mean-squares (rms) differences of bond and angle deviations were less than 0.02 Å and 3°, respectively. Rms deviations of all heavy backbone atoms from a mean structure were 0.56 ± 0.15 for residues 1–8 and 0.85 ± 0.06 for residues 1–9.

The urea planes are approximately parallel to the helix axis. The helical structure is stabilized by a number of C=O(i)···H–N′($i+2$) and C=O(i)···H–N($i+3$) H-bonds that close 12- and 14-membered rings, respectively[10]). Urea protons located near the amino terminus (N′H of residue 1 and 2 and NH of residues 2 and 3) can not be H-bonded[11]). The C=O of residue 1 is H-bonded to NH(4) and closes a 14-membered ring. In contrast, for $i=2-7$, C=O(i) is nearly equidistant from both urea protons N′H($i+2$) and NH($i+3$). Hence, intramolecular H-bonds are regularly distributed between the C=O(i) and urea N′H($i+2$) and NH($i+3$), respectively, with a frequency above 95% (*Table 6*). The C=O(i)···H–N′($i+2$) H-bond is the strongest for $i=2$, 4, and 6, whereas the C=O(i)···H–N($i+3$) H-bond dominates for $i=3$, 4, and 7. Whether this dichotomy in H-bonding strength throughout the backbone structure of **2** is a stabilizing property of the helix cannot, however, be inferred from the present study and requires the structural study of longer oligomers. In the structure of heptaurea **1**, the H-bond pattern is slightly different, the 14-membered rings being systematically more populated than the 12-membered rings.

The side chains are relatively well superimposed for all residues except aromatic ones for which multiple orientations of the ring are populated. Examination of the top view of the helix (*Fig. 7*) indicates that for $i=1-4$, side chains of residues i and $i+5$ are

[10]) Additionally, a less-frequent but still significant H-bond occurs between side chains of residues 1 and 6.

[11]) This observation is consistent with the high absolute values of temperature coefficients determined for these protons (see *Table 4*).

Table 6. *Estimated C=O(i)···H–N′(i+2) and C=O(i)···H–N(i+3) H-Bonding Pattern for* i = *1–7 Based on Statistical Analysis of the Final 20 Structures of Lowest Energy*

	C=O(*i*)···H–N′(*i*+2)			C=O(*i*)···H–N(*i*+3)		
	Frequency[a])	Distance[b])	Angle[c])	Frequency[a])	Distance[b])	Angle[c])
i=1				80	3.18±0.13	162±10
i=2	95	3.17±0.13	161±12	100	2.93±0.06	162±4
i=3	95	2.98±0.04	165±3	95	3.19±0.11	155±3
i=4	100	3.06±0.06	157±4	100	2.85±0.03	156±3
i=5	100	2.95±0.11	167±5	95	3.12±0.10	152±4
i=6	100	2.92±0.04	157±3	100	2.95±0.04	160±2
i=7	95	2.95±0.01	167±1	100[d])	3.06±0.01	158±1

[a]) Frequency of occurrence of the H-bond over the 20 lowest-energy structures, in %. An H-bond was counted when the donor-acceptor distance was less than 3.25 Å and the donor-H-acceptor angle was higher than 120°. [b]) Average O–N distance, in Å. [c]) Average O–H–N angle, in °. [d]) The terminal urea N-atom is considered here as *i*+3.

located nearly on top of each other. The distance between corresponding H–C(β)*i* and H–C(β)*i*+5 determined from an average structure is between 9.8 and 11.2 Å. With an internal diameter of *ca.* 3 Å, the helix is particularly compact and is devoid of empty volume in the interior.

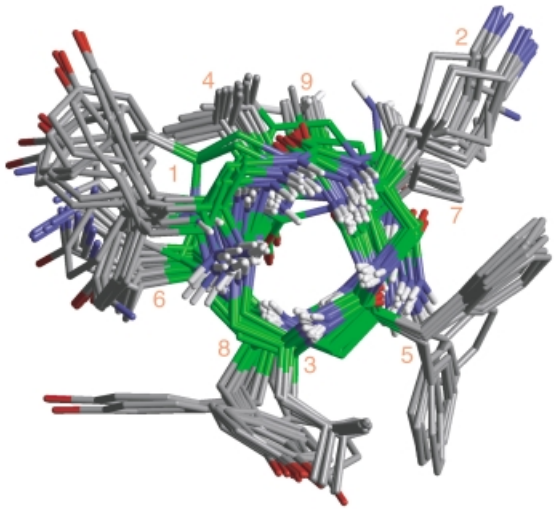

Fig. 7. *NMR Structure of oligourea* **2** *in (D$_5$)pyridine* (top view). Bundle of the 20 best structures of lowest energy.

Overlay of the structures of **1** and **2** (*Fig. 8*), both determined in (D_5)pyridine, reveals a very similar backbone conformation for the heptamer and the nonamer. The differences observed in the H-bond pattern of the two structures (*vide supra*) have little or no influence on the overall topology of the helix.

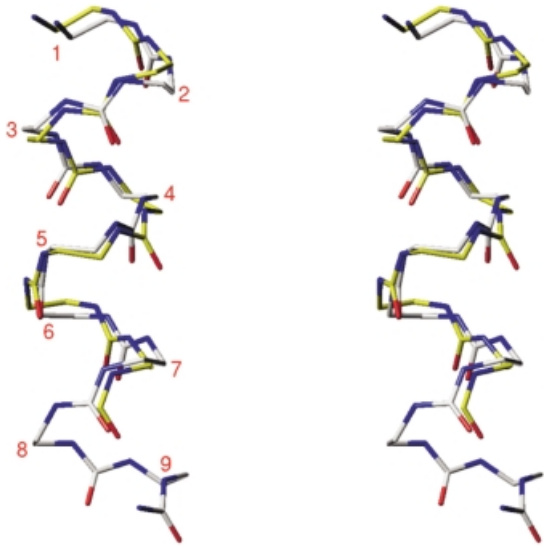

Fig. 8. *Overlay of the backbone structures of heptamer* **1** [18] *and of nonamer* **2**, *both in (D$_5$)pyridine* (stereo view). C-Atoms of the 7-mer and of the 9-mer are displayed in yellow and white, respectively. Rms deviations of all heavy backbone atoms are 0.60 Å for residues 1 – 7.

4. Circular-Dichroism Spectroscopy. – CD Spectroscopy allows the study in solution of the extrinsic asymmetry resulting from preferential conformations of optically active molecules with chromophores. Applications of this powerful technique include structural characterization of biomacromolecules (proteins, nucleic acids, polysaccharides), polypeptides constituted of α-amino acids, and, more recently, nonnatural folding oligomers [28] including β- [8] and γ-peptides [4e]. Surprisingly, experiments with γ^4-hexapeptides of type **A** (which are related to oligoureas **B** and which adopt a *2.6*$_{14}$ helical structure in CD_3OH and (D_5)pyridine [4a]) did not reveal any characteristic CD signature (no *Cotton* effect)[12]). With the aim to gain additional and complementary information about the conformation of oligoureas in solution, we have performed CD experiments with nonamer **2**. The CD Spectrum of **2** (*Fig. 9*,*a*), measured in MeOH between 194 and 250 nm at a concentration of 0.2 mM, exhibits a remarkably strong positive band at *ca.* 203 nm ($[\Phi] = +3.7 \cdot 10^5$ molar-ellipticity units) suggesting the presence of a defined secondary structure in MeOH. This CD pattern of **2** in MeOH is neither sensitive to change in concentration (data not shown) nor to increase in temperature. The intensity of the maximum at 203 nm recorded between 278.5 and 328 K decreased only slowly upon temperature increase (by less than 1% per 10 K) (*Fig. 9*,*b*). The decrease is roughly linear and does not show any melting in the temperature range studied.

---

[12]) Similarly, $\gamma^{2,4}$-peptides built from 2,4-disubstituted γ-amino acids of *like* configuration and shown to adopt a more stable *2.6* helical structure do not display typical CD curves [7a]. In contrast, CD spectra of *2.6* helical $\gamma^{2,3,4}$ peptides present a positive *Cotton* effect around 213 nm [4e].

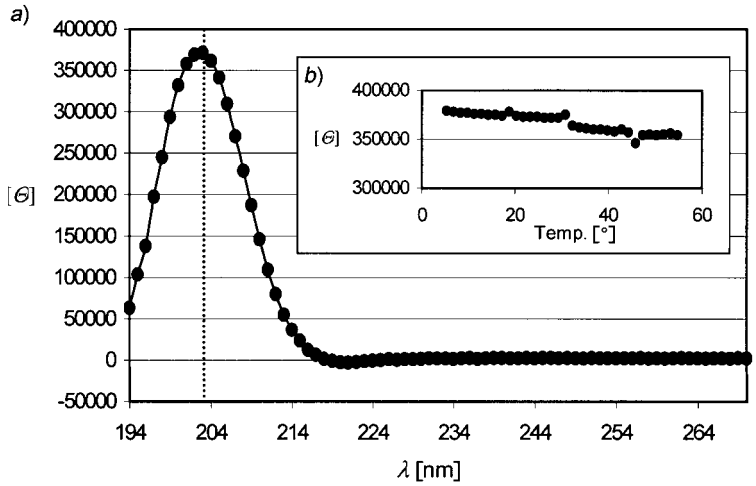

Fig. 9. *CD Analysis of oligourea* **2**: a) *CD Spectrum of* **2** *recorded in MeOH at room temperature at a concentration of* 0.2 mM. b) *CD Temperature scan of* **2** *in MeOH for* $\lambda = 203$ nm. Molar ellipticity Θ in deg · $cm^{-1} \cdot dmol^{-1}$.

5. Conclusions. – This study, which led to the NMR structure determination of nonamer **2** with Ala, Val, Leu, Phe, Tyr, and Lys side chains, further illustrates the remarkable homogeneity and stability of the *2.5* helical secondary structure adopted by enantiomerically pure *N*,*N*′-linked oligoureas **A** in pyridine. Temperature-dependent NMR experiments indicate that the helical structure is probably still present at 362 K. Comparison of the structure of nonamer **2** with the previously reported structure of heptamer **1** [18] reveals that the overall backbone traces are very similar thus suggesting that *N*,*N*′-linked oligoureas share a unique three-dimensional fold when a minimal length (still to be determined) is reached. As expected, this helix is reminiscent of the 2.6_{14} helical structure of γ-peptides. Thus, the similarity between γ-peptides and *N*,*N*′-linked oligoureas is no longer restricted to an isosteric relationship (based exclusively on the chemical formulae of the backbone) but is extended to a unique three-dimensional structural relationship.

Essentially two factors may play a role in inducing and stabilizing the *2.5* helix: *i*) a rigid (+)-*syn*-clinal arrangement around the C(α)–C(β) bond very similar to what was previously observed for β- [2e] and γ-peptides [4a][7a], and *ii*) intramolecular H-bonds. In the case of oligoureas, the helix is held by two types of H-bonds involving a given C=O, namely C=O(i)···H–N′($i+2$) and C=O(i)···H–N($i+3$) that close 12- and 14-membered H-bonded rings, respectively. In the structure of **1**, C=O(i) was not equidistant from the two urea protons[13]) and C=O(i)···H–N($i+3$) was systematically more populated than C=O(i)···H–N′($i+2$). In contrast, the two H-bonds are almost symmetrical in the modeled structure of **2**. However, in the absence of more

[13]) In the crystal structure of a *N*,*N*′-linked cyclo-tetraurea forming nanotubes, the two NH of each urea fragment are H-bonded to a C=O of a neighboring macrocycle. Interestingly, the two N···O distances are not equal, and one (3.28 Å) is just above the limit generally considered for H-bonding [19].

conclusive data, the precise position of C=O(i) relative to N′H($i+2$) and NH($i+3$) is still a matter of discussion.

Keeping in mind the absence of a characteristic CD signature for *2.6* helical γ^4-peptides, results of the first CD experiments performed on oligoureas were particularly surprising. The CD spectrum of **2** recorded in MeOH displays an intense maximum at *ca.* 203 nm (per-residue molar ellipticity: $[\Theta_r] > 40000$ deg cm^2 dmol^{-1}), which could reflect the presence of one or more regular conformations. Although it is tempting to attribute this signature to the *2.5* helical secondary structure, NMR experiments aimed at probing the occurrence of the helix in MeOH as well as CD measurements on shorter oligomers are a prerequisite, and our results along that line will be reported in due time.

Access to both the *Bruker ARX-500* facilities of the Service Commun de RMN (Faculté de Chimie, Strasbourg) and the *Bruker DRX-600*-NMR facilities of the Service Commun de Biophysicochimie des Interactions Moléculaires (Université Henri Poincaré, Nancy I) were deeply appreciated.

Experimental Part

1. *General*. Abbreviations: *GP* (general procedure), β^3-Xaa (β-homoamino acid), NMM (*N*-methylmorpholine), DMF (dimethylformamide). (D_5)Pyridine (100%, *IE* ≥ 96%) and tetramethylsilane were purchased from *Euriso-top* (France). THF was freshly distilled from Na/benzophenone under Ar before use. Toluene and pyridine were distilled from CaH_2 and stored over 4-Å molecular sieves. Amino acid derivatives and *Rink* amide resin were purchased from *Neosystem* or *Senn*. All other reagents and solvents were of anal. grade. *N*-Fmoc-β^3-amino acids bearing the Ala, Val, Leu, Phe, Tyr(O^{t}Bu), and Lys(Boc) side chains were synthesized as described starting from the corresponding *N*-Fmoc-protected α-amino acids and gave spectroscopic data in good agreement with those previously reported [24]. TLC: *Merck* silica-gel *60* F_{254} plates; detection with UV and ninhydrin. Optical rotations: 25°; *Perkin-Elmer 241* polarimeter (*Saint Quentin*, Yvelines, France). Anal. HPLC: *Beckman* instrument (*Gagny*, France); *Nucleosil-*C_{18} column 5 µm (4.6 × 150 mm); linear gradient of *A* (0.1% CF_3COOH) and *B* (MeCN containing 0.08% of CF_3COOH); flow rate 1.2 ml/min; UV detection at 214 nm; t_R in min. Prep. reversed-phase HPLC: *Perkin-Elmer* apparatus; *Aquapore ODS-20µm* column (100 × 10); linear gradient of *A* (aq. 0.06% CF_3COOH) and *B* (80% MeCN/20% *A*); flow rate 6 ml/min; UV detection at 214 nm. Circular dichroism (CD): *Jobin-Yvon CD-max6* system; recording between 190 and 300 nm; 2-mm rectangular cell; average of five scans, corrected for the baseline; oligomer concentration 0.2 mM in MeOH; molar ellipticity $[\Phi]$ in deg·cm^2·dmol^{-1} (λ in nm). NMR Spectra: *Bruker 200* (^{1}H 200 MHz, ^{13}C 50 MHz), *Bruker-Avance-300* (^{1}H 300 MHz, ^{13}C 75 MHz), *Bruker DRX-500* and *-600* spectrometers; chemical shifts δ in ppm downfield from internal $SiMe_4$ (= 0 ppm); *J* values in Hz. Matrix-assisted laser desorption/ionization (MALDI) MS: Protein TOF apparatus (*Bruker Spectrospin*, Bremen, Germany); in *m*/*z*.

2. *Succinimidyl Carbamates* **3a**–**f**: *General Procedure.* The *N*-Fmoc-β^3-amino acid (1 equiv.) was dissolved in THF (30 ml) under Ar and cooled to −20°. After addition of EtOCOCl (1.1 equiv.) and NMM (1.1 equiv.), the mixture was stirred at −20° for 20 min. The resulting white suspension was allowed to warm to −10° and treated with aq. NaN_3 soln. (5 ml; 2.5 equiv.). The mixture was stirred for 5 min, diluted with AcOEt, washed with sat. NaCl soln., dried ($MgSO_4$), and evaporated to give the expected acyl azide, which was used without further purification. Toluene was added under Ar, and the resulting soln. was heated to 65° under stirring. After the gas evolution had stopped (*ca.* 10 min), *N*-hydroxysuccinimide (1 equiv.) and pyridine (1 equiv.) were added. The mixture was stirred for 5 min at 65° and then cooled to r.t. Compounds **3a**–**f** precipitated from the toluene soln. and were collected by filtration. Recrystallization from toluene or AcOEt/^{i}Pr$_2$O afforded anal. pure monomers.

*Succinimidyl {(2*S*)-2-{[(9*H*-Fluoren-9-ylmethoxy)carbonyl]amino}propyl}carbamate* (**3a**). From Fmoc-β^3-Ala-OH (1.95 g, 6 mmol) according to the *GP*. Recrystallization from toluene yielded **3a** (2.26 g, 86%). White solid. M.p. 161–163°. $[\alpha]_D^{25} = -3.6$ ($c = 1.08$, DMF). HPLC (linear gradient, 30–100% *B*, 20 min). t_R 10.44. ^{1}H-NMR (200 MHz, CD_3CN) : 1.03 (*d*, *J* = 7, Me); 2.76 (*s*, CH_2CH_2); 2.99–3.18 (*m*, CH_2NH); 3.46–3.69 (*m*, C*H*Me); 4.18–4.34 (*m*, C*H*CH_2O); 7.22–7.45 (*m*, 4 arom. H); 7.70 (*d*, *J* = 7, 2 arom. H); 7.89 (*d*, *J* = 7, 2 arom. H); 8.33 (*t*, *J* = 6, CH_2NH). ^{13}C-NMR (50 MHz, CD_3CN): 17.8, 25.2, 45.8, 46.2, 46.7, 65.2, 120.0, 125.1, 127.0, 127.5, 140.7, 143.8, 143.9, 152.1, 155.4, 170.7. MALDI-TOF-MS: 476 ([*M* + K]$^+$), 460 ([*M* + Na]$^+$).

*Succinimidyl {(2*S*)-2-{[(9*H*-Fluoren-9-ylmethoxy)carbonyl]amino}-3-methylbutyl}carbamate* (**3b**). From Fmoc-β^3-Val-OH (3.53 g, 10 mmol) according to the *GP*. Recrystallization from toluene yielded **3b** (3.21 g, 69%). White solid. M.p. 109–111°. $[\alpha]_D^{25} = +5.9$ ($c = 1.18$, DMF). HPLC (linear gradient, 30–100% *B*, 20 min): t_R 11.84. ^{1}H-NMR (300 MHz, (D_6)DMSO): 0.90 (*d*, $J = 8$, Me); 0.95 (*d*, $J = 8$, Me); 1.72–1.89 (*m*, C*H*Me$_2$); 2.71 (*s*, CH_2CH_2); 3.08–3.42 (*m*, CH_2NH); 3.53–3.65 (*m*, NHC*H*); 4.17–4.22 (*m*, C*H*CH$_2$O); 4.35–4.51 (*m*, CHCH_2O); 6.20 (*t*, NH); 7.25–7.45 (*m*, 4 arom. H); 7.60 (*d*, $J = 7$, 2 arom. H); 7.75 (*d*, $J = 7$, 2 arom. H). ^{13}C-NMR (75 MHz, (D_6)DMSO): 18.2; 19.4; 25.4; 30.1; 44.4; 47.3; 56.7; 66.9; 120.0; 125.2; 127.1; 127.7; 141.3; 143.8; 152.2; 157.1; 169.9. MALDI-TOF-MS: 504 ([*M* + K]$^+$), 488 ([*M* + Na]$^+$).

*Succinimidyl {(2*S*)-2-{[(9*H*-Fluoren-9-ylmethoxy)carbonyl]amino}-4-methylpentyl}carbamate* (**3c**). From Fmoc-β^3-Leu-OH (2.94 g, 8 mmol) according to the *GP*. Recrystallization from toluene yielded **3c** (1.95 g, 51%). White solid. M.p. 134–137°. $[\alpha]_D^{25} = -10.8$ ($c = 1.01$, DMF). HPLC (linear gradient, 30–100% *B*, 20 min): t_R 12.63. ^{1}H-NMR (200 MHz, (D_6)DMSO): 0.80 (*d*, $J = 7$, Me); 0.83 (*d*, $J = 7$, Me); 1.14–1.33 (*m*, CH_2CHMe$_2$); 1.50–1.54 (*m*, C*H*Me$_2$); 2.57 (*s*, CH_2CH_2); 3.04–3.07 (*m*, CH_2NH); 3.51–3.58 (*m*, NHC*H*); 4.45–4.44 (*m*, C*H*CH$_2$O); 7.10 (*d*, $J = 8$, N*H*CH); 7.25–7.45 (*m*, 4 arom. H); 7.67 (*d*, $J = 7$, 2 arom. H); 7.86 (*d*, $J = 7$, 2 arom. H); 8.27 (*t*, $J = 6$, CH$_2$N*H*). ^{13}C-NMR (50 MHz, CD_3CN): 21.6; 23.3; 24.1; 25.2; 45.4; 46.8; 48.5; 65.1; 120.0; 125.1; 126.9; 127.5; 140.7; 143.7; 144.0; 152.0; 155.7; 170.7. MALDI-TOF-MS: 518 ([*M* + K]$^+$), 502 ([*M* + Na]$^+$).

*Succinimidyl {(2*S*)-2-{[(9*H*-Fluoren-9-ylmethoxy)carbonyl]amino}-3-phenylpropyl}carbamate* (**3d**). From Fmoc-β^3-Phe-OH (4.42 g, 11 mmol) according to the *GP*. Recrystallization from toluene yielded **3d** (3.73 g, 66%). White solid. M.p. 175–177°. $[\alpha]_D^{25} = -26.1$ ($c = 1.13$, DMF). HPLC (linear gradient, 30–100% *B*, 20 min). t_R 12.48 . ^{1}H-NMR (300 MHz, (D_6)DMSO): 2.55 (*s*, CH_2Ph); 2.72 (*s*, CH_2CH_2); 3.13 (*t*, $J = 6$, CH_2NH); 3.66–3.83 (*m*, NHC*H*); 4.04–4.22 (*m*, C*H*CH$_2$O); 7.06–7.43 (*m*, 9 arom. H); 7.60 (*d*, $J = 7.3$, 2 arom. H); 7.84 (*d*, $J =$ 7.7, 2 arom. H); 8.38 (*t*, $J = 5.8$, CH$_2$N*H*). ^{13}C-NMR (75 MHz, (D_6)DMSO): 25.7; 37.6; 45.2; 47.1; 52.7; 65.7; 120.5; 125.6; 126.5; 127.5; 128.0; 128.6; 128.8; 129.6; 139.0; 141.1; 144.3; 152.6; 156.0; 171.3. MALDI-TOF-MS: 552 ([*M* + K]$^+$), 536 ([*M* + Na]$^+$).

*Succinimidyl {(2*S*)-2-{[(9*H*-Fluoren-9-ylmethoxy)carbonyl]amino}-3-[4-(*tert*-butoxy)phenyl]propyl}carbamate* (**3e**). From Fmoc-β^3-Tyr(^{t}Bu)-OH (2.37 g, 5 mmol) according to the *GP*. Recrystallization from toluene yielded **3e** (2.28 g, 78%). White solid. M.p. 138–140°. $[\alpha]_D^{25} = -22.9$ ($c = 1.12$, DMF). HPLC (linear gradient, 30–100% *B*, 20 min): t_R 13.87. ^{1}H-NMR (300 MHz, (D_6)DMSO): 1.13 (*s*, ^{t}Bu); 2.48–2.69 (*m*, CH_2Ar); 2.72 (*s*, CH_2CH_2); 3.13 (*t*, $J = 6$, CH_2NH); 3.63–3.82 (*m*, NHC*H*); 4.02–4.23 (*m*, C*H*CH$_2$O); 6.74 (*d*, $J = 8$, 2 arom. H); 7.06 (*d*, $J = 8$, 2 arom. H); 7.22–7.42 (*m*, 4 arom. H); 7.57–7.66 (*m*, 2 arom. H); 7.84 (*d*, $J = 7$, 2 arom. H); 8.38 (*t*, $J = 6$, CH$_2$N*H*). ^{13}C-NMR (75 MHz, (D_6)DMSO): 24.5; 27.7; 35.9; 44.1; 45.9; 51.5; 64.6; 76.7; 119.3; 122.6; 122.7; 124.5; 126.3; 126.8; 128.8; 132.3; 140.0; 143.1; 151.4; 152.5; 154.8; 170.1. MALDI-TOF-MS: 624 ([*M* + K]$^+$), 608 ([*M* + Na]$^+$).

*Succinimidyl {(2*S*)-2-{[(9*H*-Fluoren-9-ylmethoxy)carbonyl]amino}-6-{[(tert-butoxy)carbonyl]amino}hexyl}carbamate* (**3f**). From Fmoc-β^3-Lys(Boc)-OH (7.16 g, 13 mmol) according to the *GP*. Recrystallization from toluene yielded **3f** (6.81 g, 79%). White solid. M.p. 122–124°. $[\alpha]_D^{25} = -4.7$ ($c = 1.16$, DMF). HPLC (linear gradient, 30–100% *B*, 20 min): t_R 12.67. ^{1}H-NMR (300 MHz, (D_6)DMSO): 1.09–1.45 (*m*, O^{t}Bu, (CH$_2$)$_3$); 2.71 (*s*, CH_2CH_2); 2.79–2.95 (*m*, CH_2NH); 3.30–3.32 (*m*, CH_2NH); 3.46–3.50 (*m*, NHC*H*); 4.16–4.29 (*m*, C*H*CH$_2$O); 6.71 (*t*, $J = 6$, NH); 7.12 (*d*, $J = 7$, NH); 7.27–7.42 (*m*, 4 arom. H); 7.64–7.69 (*d*, $J = 7$, 2 arom. H); 7.85 (*d*, $J = 7$, 2 arom. H); 8.27 (*t*, $J = 6$, CH$_2$N*H*). ^{13}C-NMR (75 MHz, (D_6)DMSO): 22.7; 25.2; 28.2; 29.4; 31.0; 39.8; 45.0; 46.8; 50.5; 65.2; 77.3; 120.0; 125.2; 127.0; 127.5; 140.7; 143.8; 152.0; 155.5; 170.8. MALDI-TOF-MS: 702 ([*M* + K]$^+$), 686 ([*M* + Na]$^+$).

3. *Oligourea* **2**. Assembly of the protected oligourea chain was carried out with a homemade multichannel synthesizer [29] in a semi-automatic mode on a 50-μmol scale starting from *Rink* amide resin (0.62 mmol/g). The Fmoc group at the starting resin was removed with 20% piperidine in DMF (3 × 5 min) under N_2 bubbling. The resin was then filtered and washed with DMF (5 × 1 min). For each coupling step, a soln. of the carbamate **3a–f** (5 equiv.) in DMF and NMM (2 equiv.) were added successively to the resin, and the suspension was mixed under N_2 bubbling for 70 min. A double coupling was performed systematically. Monitoring of the coupling reaction was generally performed with the *Kaiser* ninhydrin test [30] or with 2,4,6-trinitrobenzenesulfonic acid [31]. After the removal of the last Fmoc protecting group, the resin was washed with CH_2Cl_2 and Et_2O and dried under N_2. Side-chain deprotection and cleavage of the oligomer from the resin was performed by treatment with CF_3COOH/H_2O for 150 min at 20°. After precipitation in cold Et_2O and centrifugation, the crude oligomer was solubilized and lyophilized to afford crude **2** as CF_3COOH salt (90 mg, quant.), purity 32% (reversed-phase HPLC). The crude oligomer was finally purified by reversed-phase HPLC (linear gradient, 0–80% *B*, 40 min)

and lyophilized to give **2** as a CF_3COOH salt (16 mg, 18%). White solid. HPLC (linear gradient, 5–65% *B*, 20 min): t_R 14.95. ^{1}H-NMR (500 MHz, (D_5)pyridine): *Table 1*. MALDI-TOF-MS: 1393.0 ($[M+1]^+$).

4. *NMR Spectroscopy of Oligourea* **2**. Spectra were recorded with *Bruker DRX-500* and *-600* NMR spectrometers by means of 5 mm inverse 1 H/*X* with *Z* gradient capabilities probes. The temperature was maintained at 308 K for the structure determination. 1) DQF-COSY [32] was performed by a gradient-selection pathway. Acquisition: $2K(t_2)\cdot 512(t_1)$ data points; relaxation delay of 3 s; QF mode in t_1 and 2 scans per increment. Processing was done after a sine-bell $\Pi/3$-shifted multiplication in both dimensions, and *Fourier* transformed in $1K\cdot 1K$ real data points. 2) TOCSY [33] plots were recorded with $2K(t_2)\cdot 512(t_1)$ data points in echo-antiecho mode with *Z*-gradients selection; relaxation delay of 3 s and 16 scans per increments; two experiments were recorded with mixing times of 124 and 70 ms, resp. Processing: Zero-filling and FT to $2K\cdot 2K$ after multiplication by cosine in both dimensions. 3) An adiabatic off-resonance ROESY [34] was recorded with $2K(t_2)\cdot 512(t_1)$ data points; acquisition in states-TPPI mode; 8 scans per increment and 3 s relaxation delay. The CW-spin lock field of 5 KHz was alternatively shifted by $+/-3750$ Hz to achieve a $\mathrm{tg}(\theta)=54.7^\circ$ allowing an efficient mismatch of the *Hartmann-Hahn* condition. The adiabatic pulse was a trapezoidal shape. The mixing time was 300 ms. Processing was done with $1K\cdot 1K$ real data points after multiplication by cosine filters in both dimensions. 4) Several 2D-NOESY experiments with mixing times from 200 to 500 ms were also performed with $2K(t_2)\cdot 512(t_1)$ data points in states-TPPI mode with *Z*-gradients selection; relaxation delay of 1.5 s and 96 scans per increments. The build-up curve for different NOE correlations showed that spin diffusion was negligible for $\tau_m=300$ ms. The adiabatic off-resonance ROESY experiment appeared more sensitive and was used for the structure determination.

The spectral width in F_1 was 5000 Hz. Data processing was performed with XWIN-NMR software. The intensity of peaks was extracted from the ROESY plot with Sparky software [35] and the interproton distances calculated taking as reference the distance of 1.78 Å between the different sets of C(α) protons. Distance restraints were assigned as strong, medium, and weak, and set at intervals of 1.8–2.8, 2.8–3.8, and 3.8–5.5 Å, resp.

5. *Structure of Oligourea* **2**. All calculations were performed with the AMBER6 suite of programs [36]. Parameters and topology files were first generated for each residue by a previously described procedure [37]. Starting from a fully extended structure generated by the SYBYL 6.8 package [38], geometries and atomic charges were calculated with the GAUSSIAN98 program [39] by means of the HF/6-31G* basis set. Therein, atom-centered charges were fitted to an *ab initio* electrostatic potential with the RESP method [40]. With SYBYL, 30 starting structures were randomly generated; they were further energy-minimized (1000 steps steepest descent followed by 1000 steps conjugate gradient relaxation) with AMBER6 by means of the *Cornell* force-field [41]. The *ab initio* simulated annealing protocol started for each conformation with a 75-ps high-temperature phase at 600 K followed by a 25-ps cooling phase where the temperature was linearly lowered from 600 to 1 K. During the first 75 ps, the NMR restraints (103 NOE-derived intraresidue restraints, 21 inter-residue distance restraints, 38 torsional angle restraints) were slowly turned on, and fully effective during the cooling phase. NMR Restraints were treated with the sander potential by means of 4 boundaries for each restraint. The penalty function is flat (equal to zero) between an inner set of upper and lower bounds (2.3–2.8, 3.3–3.8, and 5.0–5.5 for strong, medium and weak NOEs, resp.), then rises parabolically when the internal coordinates violate these bounds, and are finally linear outside even wider upper and lower bounds (1.8–3.3, 2.8–3.3, and 4.0–6.0 for strong, medium, and weak NOEs, resp.).Torsional-angle restraints were assigned similarly with 4 bounds ($\tau-40$, $\tau-20$, $\tau+20$, and $\tau+40$ for a torsion to which an average value of τ was measured). For all restraints, a force constant of 32 $\mathrm{kcal\cdot mol^{-1}\cdot \AA^{-2}}$ and 50 $\mathrm{kcal\cdot mol^{-1}\cdot rad^{-2}}$ was assigned from distance and torsional-angles restraints, resp. The resulting structures were analyzed in terms of deviations to experimental restraints (no NOE violations >0.50 Å and no dihedral-angle violation $>10^\circ$). The final 20 structures with the lowest energy were used for the structural statistics.

REFERENCES

[1] D. J. Hill, M. J. Mio, R. B. Prince, T. S. Hughes, J. S. Moore, *Chem. Rev.* **2001**, *101*, 3893; M. S. Cubberley, B. L. Iverson, *Curr. Opin. Chem. Biol.* **2001**, *5*, 650; K. D. Stigers, M. J. Sothn J. S. Nowick, *Curr. Opin. Chem. Biol.* **1999**, *3*, 714; K. Kirshenbaum, R. N. Zuckermann, K. A. Dill, *Curr. Opin. Struct. Biol.* **1999**, *9*, 530; S. H. Gellman, *Acc. Chem. Res.* **1998**, *31*, 173.

[2] a) D. Seebach, M. Overhand, F. N. M. Kühnle, B. Martinoni, L. Oberer, U. Hommel, H. Widmer, *Helv. Chim. Acta* **1996**, *79*, 913; b) D. Seebach, P. E. Ciceri, M. Overhand, B. Jaun, D. Rigo, L. Oberer, U.

Hommel, R. Amstutz, H. Widmer, *Helv. Chim. Acta* **1996**, *79*, 2043; c) D. Seebach, S. Abele, K. Gademann, G. Guichard, T. Hintermann, B. Jaun, J. L. Matthews, J. V. Schreiber, L. Oberer, U. Hommel, H. Widmer, *Helv. Chim. Acta* **1998,** *79*, 932; d) S. Abele, G. Guichard, D. Seebach, *Helv. Chim. Acta* **1998**, *81*, 2141; e) Karl Gademann, B. Jaun, D. Seebach, R. Perozzo, L. Scapozza, G. Folkers, *Helv. Chim. Acta* **1999**, 82, 1; d) D. Seebach, T. Sifferlen, P. A. Mathieu, A. M. Häne, C. M. Krell, D. J. Bierbaum, S. Abele, *Helv. Chim. Acta* **2000**, 83, 2849.

[3] D. Seebach, S. Abele, Karl Gademann, B. Jaun, *Angew. Chem.* **1999**, *111*, 1700; *Angew. Chem., Int. Ed.* **1999**, *38*, 1595.

[4] a) T. Hintermann, K. Gademann, B. Jaun, D. Seebach, *Helv. Chim. Acta* **1998**, *81*, 983; b) D. Seebach, M. Brenner, M. Rueping, B. Schweizer, B. Jaun, *Chem. Commun.* **2001**, 207; c) M. Brenner, D. Seebach, *Helv. Chim. Acta* **2001**, 84, 1181; d) M. Brenner, D. Seebach, *Helv. Chim. Acta* **2001**, 84, 2155; e) D. Seebach, M. Brenner, M. Rueping, B. Jaun, *Chem. – Eur. J.* **2002**, *8*, 573.

[5] H. Appella, L. A. Christianson, I. L. Karle, D. R. Powell, S. H. Gellman, *J. Am. Chem. Soc.* **1996**, *118,* 13071; D. H. Appella, L. A. Christianson, D. A. Klein, D. R. Powell, X. Huang, J. J. Barchi Jr., S. H. Gellman, *Nature* (London) **1997**, *387*, 381; D. H. Appella, J. J. Barchi Jr., S. R. Durell, S. H. Gellman, *J. Am. Chem. Soc.* **1999**, *121*, 2309; X. Wang, J. F. Espinosa, S. H. Gellman, *J. Am. Chem. Soc.* **2000**, *122,* 4821.

[6] S. Krauthäuser, L. A. Christianson, D. R. Powell, S. H. Gellman, *J. Am. Chem. Soc.* **1997**, *119*, 11719; Y. J. Chung, R. B. R. Huck, L. A. Christianson, H. E. Stanger, S. Krauthäuser, D. R. Powell, S. H. Gellman, *J. Am. Chem. Soc.* **2000**, *122*, 3995.

[7] a) S. Hanessian, X. Luo, R. Schaum, S. Michnick, *J. Am. Chem. Soc.* **1998**, *120*, 8569; b) S. Hanessian, X. Luo, R. Schaum, *Tetrahedron Lett.* **1999**, *40*, 4925.

[8] D. Seebach, J. L. Matthews, *Chem. Commun.* **1997,** *21*, 2015; R. P. Cheng, S. H. Gellman, W. F. DeGrado, *Chem. Rev.* **2001,** 101, 3219.

[9] C. Muller, E. Kitas, H. P. Wessel, *J. Chem. Soc., Chem. Commun.* **1995**, *23*, 2425; L. Szabo, B. L. Smith, K. D. McReynolds, A. L. Parrill, E. R. Morris, J. Gervay, *J. Org. Chem.* **1998**, *63*, 1074; M. D. Smith, D. D. Long, T. D. W. Claridge, D. G. Marquess, G. W. J. Fleet, *J. Chem. Soc., Chem. Commun.* **1998**, *18*, 2039; D. D. Long, M. D. Smith, D. G. Marquess, T. D. W. Claridge, G. W. J. Fleet, *Tetrahedron Lett.* **1998**, *39*, 9293.

[10] K. Kirshenbaum, A. E. Barron, R. A. Goldsmith, P. Armand, E. K. Bradley, K. T. Truong, K. A. Dill, F. E. Cohen, R. N. Zuckermann, *Proc. Natl. Acad. Sci. USA* **1998,** *95*, 4303; C. W. Wu, T. J. Sanborn, R. N. Zuckermann, A. E. Barron, *J. Am. Chem. Soc.* **2001,** 123, 2958; C. W. Wu, T. J. Sanborn, K. Huang, R. N. Zuckermann, A. E. Barron, *J. Am. Chem. Soc.* **2001,** *123*, 6778.

[11] F. Bernardi, M. Garavelli, M. Scatizzi, C. Tomasini, V. Trigari, M. Crisma, F. Formaggio, C. Peggion, C. Toniolo, *Chem. – Eur. J.* **2002**, *8*, 2516.

[12] D. Yang, J. Qu, B. Li, F.-F. Ng, X.-C. Wang, K.-K. Cheung, D.-P. Wang, Y.-D. Wu, *J. Am. Chem. Soc.* **1999**, *121*, 589.

[13] H. Han, K. D. Janda, *J. Am. Chem. Soc.* **1996,** *118,* 2539.

[14] a) R. Günther, H.-J. Hoffmann, *J. Am. Chem. Soc.* **2001**, *123*, 247; b) G. Lelais, D. Seebach, 'Proceedings of the 2nd International and the 17th American Peptide Symposium – San Diego (June 2001)', in 'Peptides: The Wave of the Future', Eds. M. Lebl and R. A. Houghten, American Peptide Society, San Diego, 2001, p. 581.

[15] K. Burgess, D. S. Linthicum, H. Shin, *Angew. Chem., Int. Ed.* **1995**, *34*, 907; K. Burgess, J. Ibarzo, D. S. Linthicum, D. H. Russell, H. Shin, A. Shitangkoon, R. Totani, A. J. Zhang, *J. Am. Chem. Soc.* **1997**, *119*, 1556.

[16] C. Y. Cho, E. J. Moran, S. R. Cherry, J. C. Stephans, S. P. A. Fodor, C. L. Adams, A. Sundaram, J. W. Jacobs, P. G. Schultz, *Science (Washington, D.C.)* **1993**, *261*, 1303; C. Y. Cho, R. S. Youngquist, S. J. Paikoff, M. H. Beresini, A. R. Herbert, L. T. Berleau, C. W. Liu, D. E. Wemmer, T. Keough, P. G. Schultz, *J. Am. Chem. Soc.* **1998**, *120*, 7706.

[17] V. Semetey, D. Rognan, C. Hemmerlin, C. Didierjean, A.-P. Schaffner, A. Gimenez Giner, A. Aubry, J.-P. Briand, M. Marraud, G. Guichard, *Org. Lett.* **2001**, *3*, 3843.

[18] V. Semetey, D. Rognan, C. Hemmerlin, R. Graff, J.-P. Briand, M. Marraud, G. Guichard, *Angew. Chem.* **2002**, *115*, 1973; *Angew. Chem., Int. Ed.* **2002**, *41*, 1893.

[19] V. Semetey, C. Didierjean, J.-P. Briand, A. Aubry, G. Guichard, *Angew. Chem.* **2002**, *115*, 1975; *Angew. Chem., Int. Ed.* **2002**, *41*, 1895.

[20] J. M. Kim, Y. Bi, S. Paikoff, P. G. Schultz, *Tetrahedron Lett.* **1996**, *37*, 5305.

[21] A. Boeijen, R. M. J. Liskamp, *Eur. J. Org. Chem.* **1999**, 2127.

[22] G. Guichard, V. Semetey, C. Didierjean, A. Aubry, J. P. Briand, M. Rodriguez, *J. Org. Chem.* **1999**, *64*, 8702.

[23] G. Guichard, V. Semetey, M. Rodriguez, J. P. Briand, *Tetrahedron Lett.* **2000**, *41*, 1553.
[24] G. Guichard, S. Abele, D. Seebach, *Helv. Chim. Acta* **1998**, *81*, 187.
[25] H. Rink, *Tetrahedron Lett.* **1987**, *37*, 3787.
[26] H. Kessler, *Angew. Chem., Int. Ed.* **1982**, *21*, 512.
[27] K. D. Kopple, M. Ohnishi, A. Go, *J. Am. Chem. Soc.* **1969,** *91*, 4264; N. H. Andersen, J. W. Neidigh, S. M. Harris, G. M. Lee, Z. Liu, H. Tong, *J. Am. Chem. Soc.***1997,** *119*, 8547.
[28] K. D. McReynolds, J. Gervay-Hague, *Tetrahedron: Asymmetry* **2000**, *11*, 337.
[29] J. Neimark, J.-P. Briand, *Peptide Res.* **1993**, *6*, 219.
[30] E. Kaiser, R. L. Colescott, C. D. Bossinger, P. I. Cook, *Anal. Biochem.* **1970**, *34*, 595.
[31] W. S. Hancok, J. E. Battersby, *Anal. Biochem.* **1976**, *71*, 260.
[32] R. R. Ernst, *Chem. Phys. Lett.* **1977**, *52* , 407; B. Ancian, I. Bourgeois, J.-F. Dauphin, A. A. Shaw, *J. Magn. Reson. A* **1997**, *125*, 348. A. Wokaun
[33] A. Bax, D. G. Davis, *J. Magn. Reson.* **1985**, *65*, 355.
[34] A. Bax, D. G. Davis, *J. Magn. Reson.* **1985**, *63*, 207; H. Desvaux, P. Berthault, N. Birlirakis, M. Goldman, M. Piotto, *J. Magn. Reson. A* **1995**, *113*, 47.
[35] T. D. Goddard, D. G. Kneller, 'Sparky 3', University of California, San Francisco.
[36] D. A. Case, D. A. Pearlman, J. W. Caldwell, D. E. Cheatham III, W. S. Ross, C. L. Simmerling, T. A. Darden, K. M. Merz, R. V. Stanton, A. L. Cheng, J. J. Vincent, M. Crowley, V. Tsui, R. J. Radmer, Y. Duan, J. Pitera, I. Massova, G. L. Seibel, U. C. Singh, P. K. Weiner, P. A. Kollman, 'AMBER6', University of California, San Francisco, 1999.
[37] D. Rognan, S. Mukhija, G. Folkers, O. Zerbe, *J. Comput.-Aided Mol. Design* **2001** *15*, 103.
[38] SYBYL6.8, Tripos Inc., St. Louis, Missouri, MO 63144, USA.
[39] GAUSSIAN 98, Revision A.9, M. J. Frisch, G. W. Trucks, H. B. Schlegel, G.E. Scuseria, M. A. Robb, J. R. Cheeseman, V. G. Zakrzewski, J. A. Montgomery Jr., R. E. Stratmann, J. C. Burant, S. Dapprich, J. M. Millam, A. D. Daniels, K. N. Kudin, M. C. Strain, O. Farkas, J. Tomasi, V. Barone, M. Cossi, R. Cammi, B. Mennucci, C. Pomelli, C. Adamo, S. Clifford, J. Ochterski, G. A. Petersson, P. Y. Ayala, Q. Cui, K. Morokuma, D. K. Malick, A. D. Rabuck, K. Raghavachari, J. B. Foresman, J. Cioslowski, J. V. Ortiz, A. G. Baboul, B. B. Stefanov, G. Liu, A. Liashenko, P. Piskorz, I. Komaromi, R. Gomperts, R. L. Martin, D. J. Fox, T. Keith, M. A. Al-Laham, C. Y. Peng, A. Nanayakkara, M. Challacombe, P. M. W. Gill, B. Johnson, W. Chen, M. W. Wong, J. L. Andres, C. Gonzalez, M. Head-Gordon, E. S. Replogle, J. A. Pople, Gaussian, Inc., Pittsburgh PA, 1998.
[40] C. I. Bayly, P. Cieplak, W. D. Cornell, P. A. Kollman, *J. Phys. Chem.* **1993**, *97*, 10269.
[41] W. D. Cornell, P. Cieplak, C. I. Bayly, I. R. Gould, K. Merz Jr., D. M. Ferguson, D. C. Spellmeyer, T. Fox, J. W. Caldwell, P. A. Kollman, *J. Am. Chem. Soc.* **1995**, *117*, 5179.

Received June 7, 2002